

Supplementary Information for:

## **Nucleotide binding halts diffusion of the eukaryotic replicative helicase during activation**

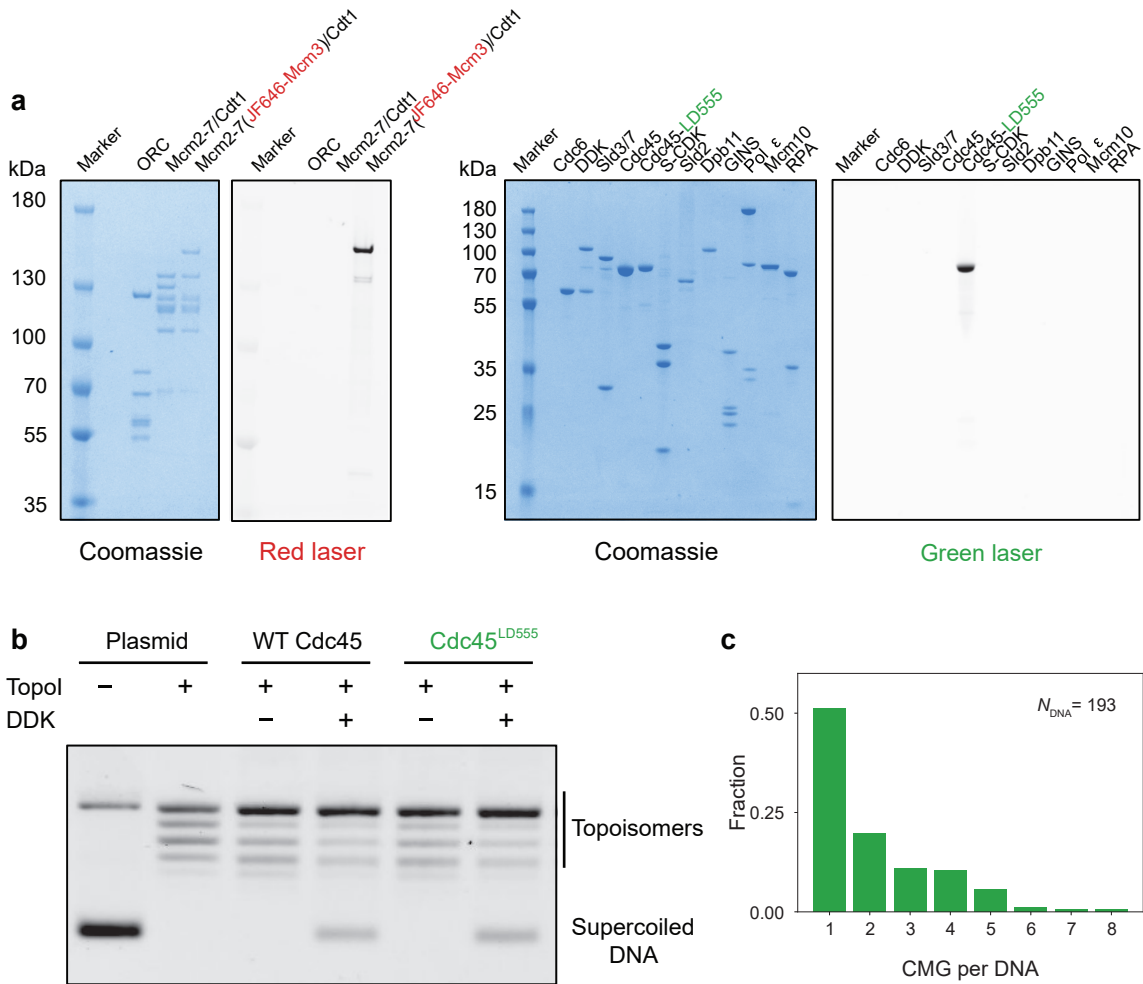
Daniel Ramírez Montero<sup>1</sup>, Humberto Sánchez<sup>1</sup>, Edo van Veen<sup>1</sup>, Theo van Laar<sup>1</sup>, Belén Solano<sup>1</sup>, John F. X. Diffley<sup>2\*</sup>, and Nynke H. Dekker<sup>1\*</sup>.

<sup>1</sup>Department of Bionanoscience, Kavli Institute of Nanoscience, Delft University of Technology, Delft, The Netherlands.

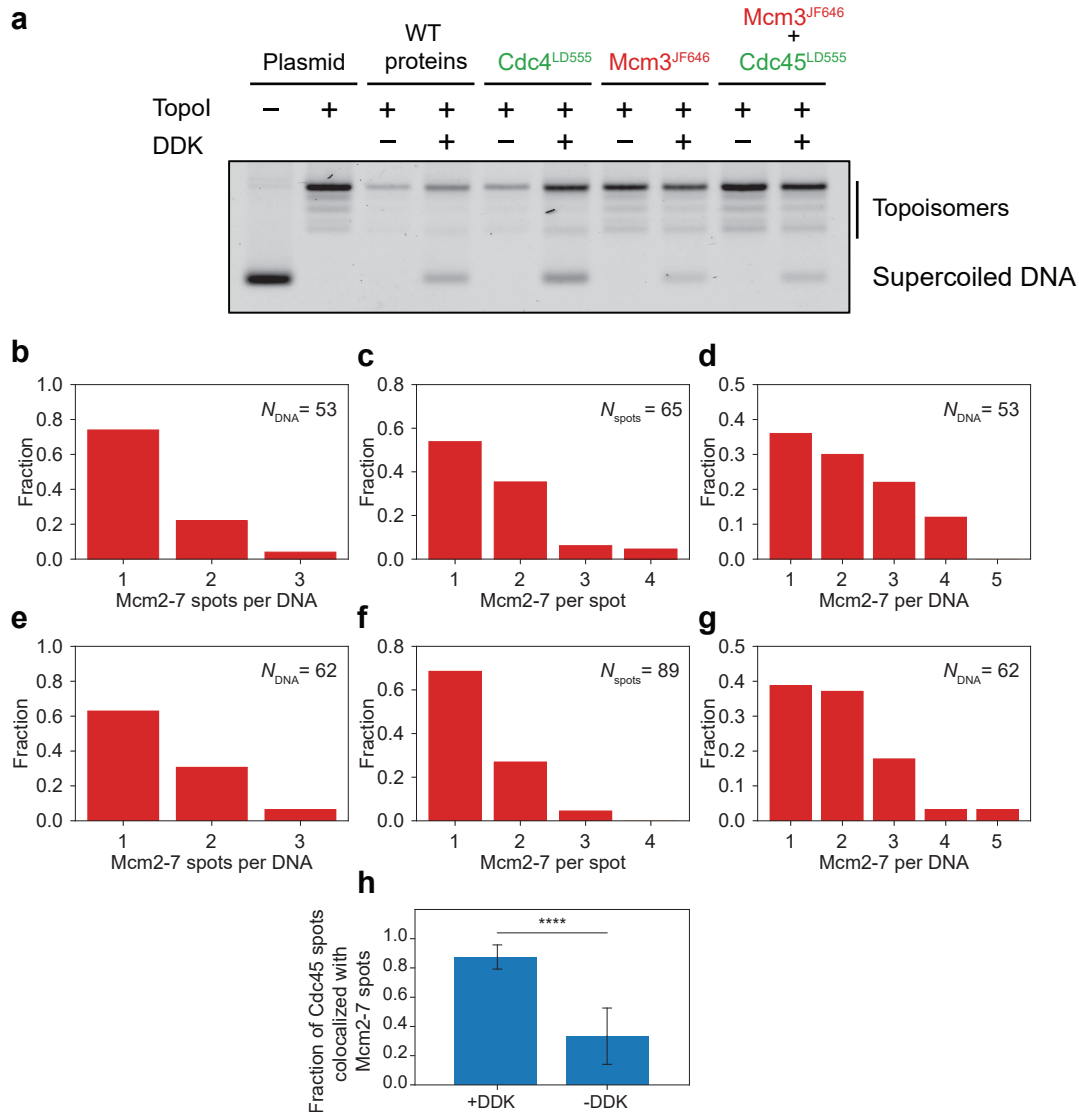
<sup>2</sup>Chromosome Replication Laboratory, Francis Crick Institute, London, UK.

\*Correspondence: [john.diffley@crick.ac.uk](mailto:john.diffley@crick.ac.uk); [n.h.dekker@tudelft.nl](mailto:n.h.dekker@tudelft.nl)

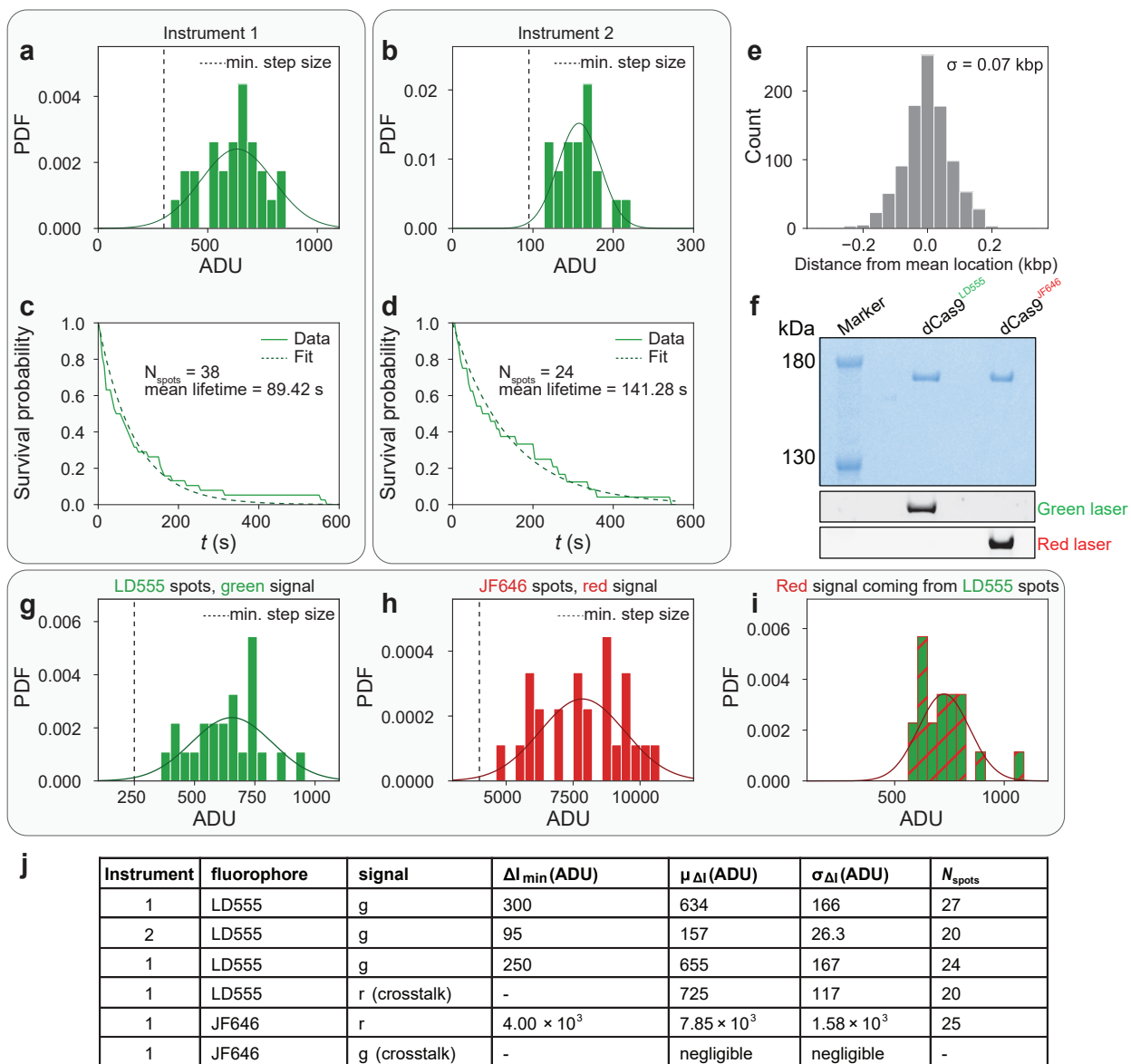
## Supplementary Figures:



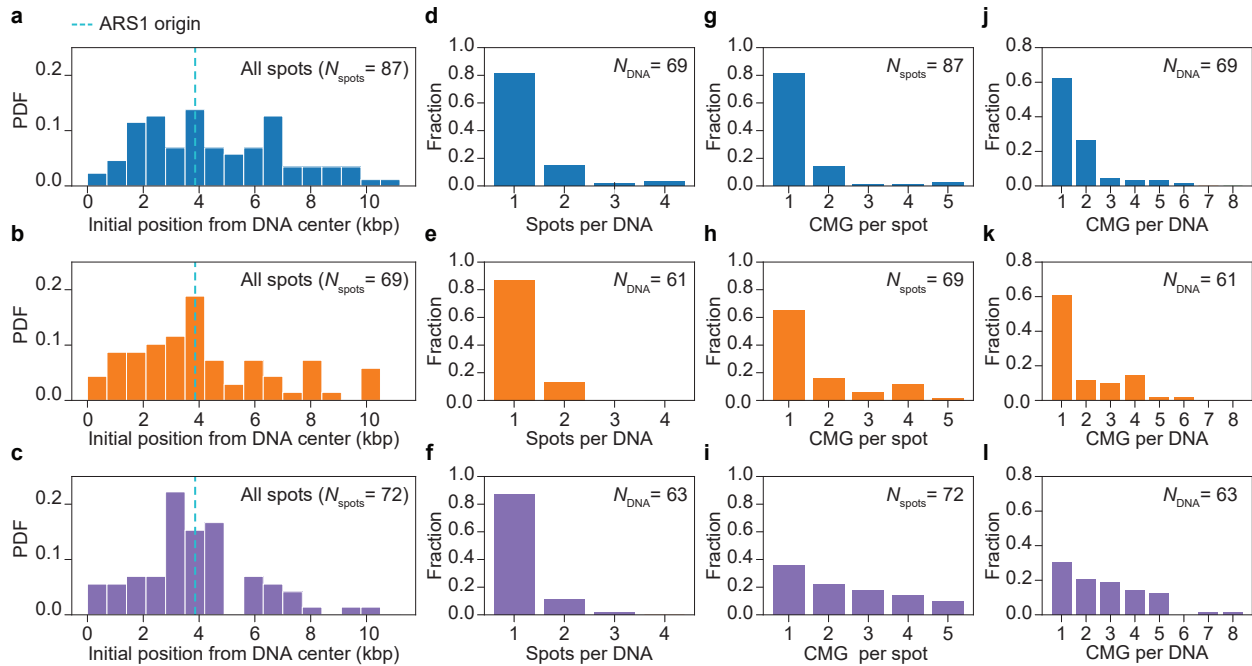
**Supplementary Figure 1 | Hybrid ensemble and single-molecule assay and reagent validation.** **a**, SDS-PAGE showing the minimal set of purified proteins required for the reconstitution of CMG assembly and activation; the gels were stained with Coomassie Blue Stain and fluorescently scanned with either a red or a green laser, to show the fluorescently labeled proteins in either color. **b**, Ensemble unwinding assay showing that Cdc45<sup>LD555</sup> supports DNA unwinding to near WT levels ( $N=2$  biological replicates). **c**, Distribution of total numbers of fluorescent CMG complexes per DNA, obtained by combining the total number of CMG diffraction-limited spots per DNA (Fig. 1b) with the number of CMG complexes within each spot (Fig. 1c). Source data are provided as a Source Data file.



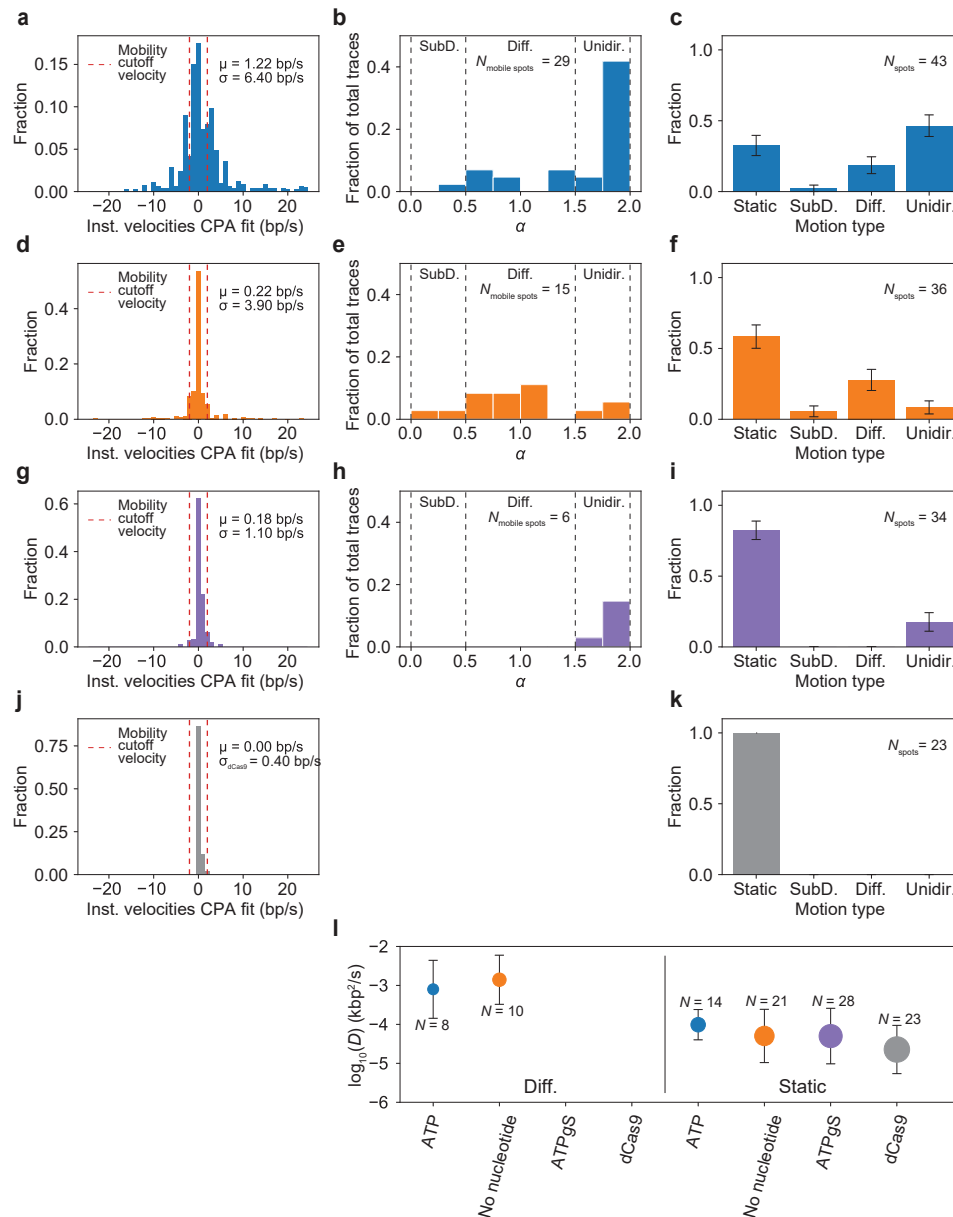
**Supplementary Figure 2 | Reagent validation, distribution of number of Mcm2-7 spots and distribution of Mcm2-7 complexes within each spot.** **a**, Ensemble unwinding assay showing that Mcm2-7<sup>JF646</sup> supports DNA unwinding alone and in conjunction with Cdc45<sup>LD555</sup> ( $N=1$  biological replicate). **b**, Distribution of the number of Mcm2-7 diffraction-limited spots per DNA in the presence of DDK. **c**, Distribution of the number of Mcm2-7 complexes within each diffraction-limited spot in the presence of DDK. **d**, Distribution of the total number of Mcm2-7 complexes per DNA molecule in the presence of DDK, obtained by combining data from **b** and **c**. **e**, Distribution of the number of Mcm2-7 diffraction-limited spots per DNA in the absence of DDK. **f**, Distribution of the number of Mcm2-7 complexes within each diffraction-limited spot in the absence of DDK. **g**, Distribution of the total number of Mcm2-7 complexes per DNA molecule in the absence of DDK, obtained by combining data from **e** and **f**. **h**, Mean fraction of Cdc45<sup>LD555</sup> diffraction-limited spots that are colocalized with Mcm2-7<sup>JF646</sup> diffraction-limited spots in the presence ( $N_{\text{Cdc45 spots}}=16$ ) or absence ( $N_{\text{Cdc45 spots}}=6$ ) of DDK; error bars show the standard error of proportion. Statistical significance was obtained from a two-sided binomial test ( $p\text{-value}=1.2 \times 10^{-5}$ ). Source data are provided as a Source Data file.



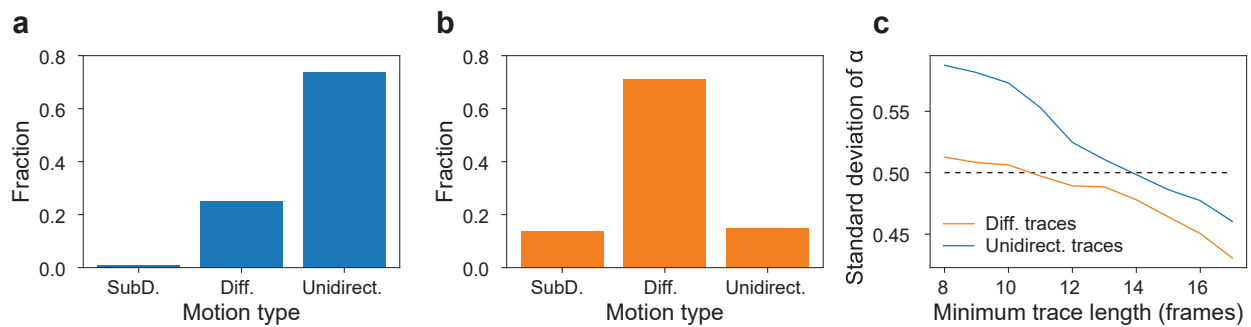
**Supplementary Figure 3 | Fluorescently labeled dCas9 proteins as standards for determination of number of proteins per diffraction-limited spot and localization accuracy.** **a-b**, Distribution of photobleaching step sizes of fluorescently labeled dCas9<sup>LD555</sup> imaged under the same imaging conditions as fluorescent CMG in the single-color experiments; **a**, and **b**, correspond to the two instruments used in this study; both distributions were fitted to a normal distribution;  $\mu - 2\sigma$  was used as the minimum step size in the single-color CMG experiments to capture at least 95 % of bleaching events. **c-d**, Distribution of times to photobleaching of fluorescently labeled dCas9<sup>LD555</sup> imaged under the same imaging conditions as fluorescent CMG; **c**, and **d**, correspond to the two instruments used in this study; both distributions were fitted to a single exponential decay. **e**, distribution of positional measurements of fluorescently labeled dCas9<sup>LD555</sup>; as dCas9<sup>LD555</sup> is expected to be static, the standard deviation of this distribution gives us the localization error in our experiments. **f**, SDS-PAGE of dCas9 with fluorescently labeled with dyes LD555, JF646, respectively; the gel was stained with Coomassie Blue stain and fluorescently scanned with a red, green laser, respectively. **g**, Distribution of photobleaching step sizes of fluorescently labeled dCas9<sup>LD555</sup> when simultaneously excited with the green and red lasers in instrument 1, as done in the Mcm2-7 and Cdc45 colocalization experiments; the distribution was fitted to a normal distribution;  $\mu - 2\sigma$  was used as the minimum step size in the dual-color CMG experiments to capture at least 95 % of bleaching events. **h**, Distribution of photobleaching step sizes of fluorescently labeled dCas9<sup>JF646</sup> when simultaneously excited with the green and red lasers in instrument 1, as done in the Mcm2-7 and Cdc45 colocalization experiments; the distribution was fitted to a normal distribution;  $\mu - 2\sigma$  was used as the minimum step size in the dual-color CMG experiments to capture at least 95 % of bleaching events. **i**, Distribution of red signal coming from green fluorescently labeled dCas9<sup>LD555</sup> when simultaneously excited with the green and red lasers in instrument 1, as done in the Mcm2-7 and Cdc45 colocalization experiments. The distribution was fitted to a normal distribution and the mean value was used for crosstalk corrections. **j**, Summary table of all the parameters obtained from **a-e**, and **g-i**. Source data are provided as a Source Data file.



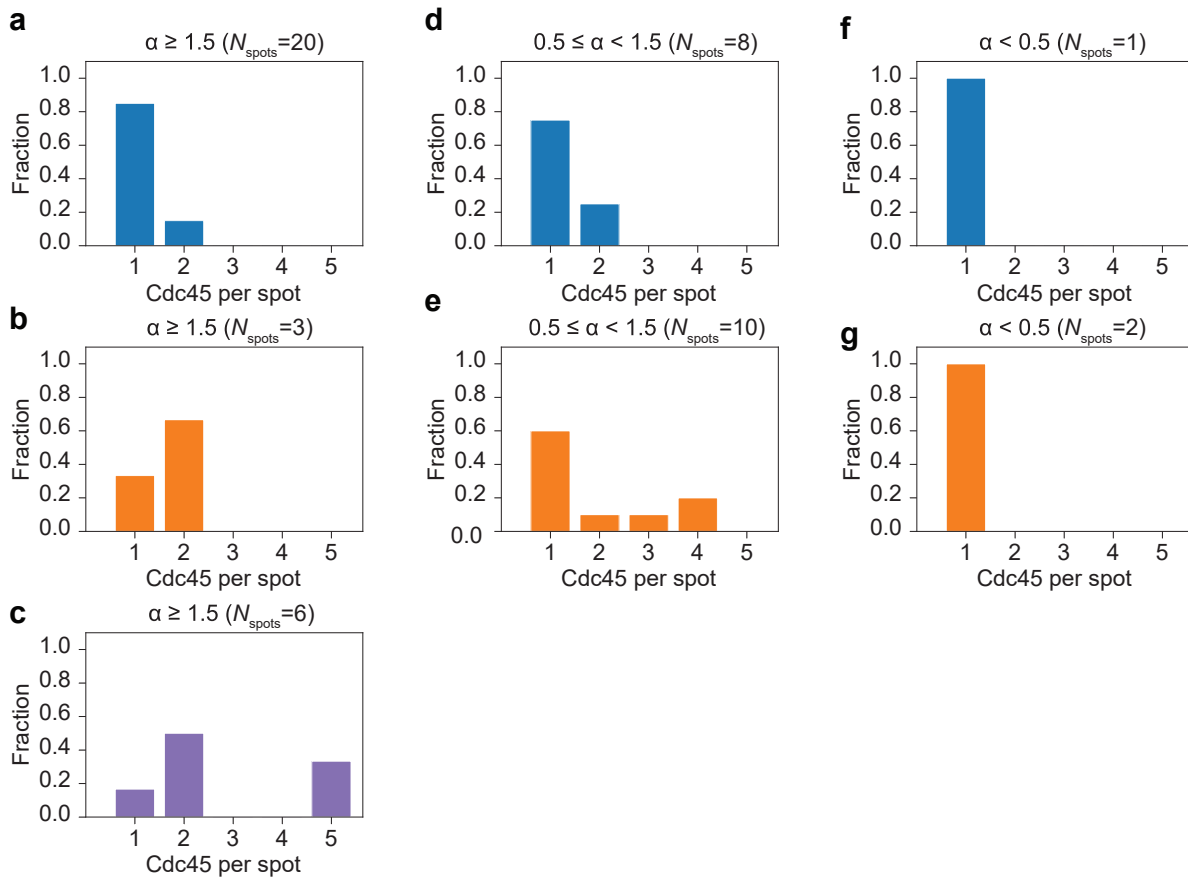
**Supplementary Figure 4 | Distribution of initial positions, numbers of CMG spots and numbers of CMG complexes within each spot for the different biochemical conditions tested. a-c,** Distribution of initial positions on the DNA of all Cdc45 diffraction-limited spots for DNA molecules imaged in **a**, the presence of ATP, **b**, the absence of nucleotide or, **c**, the presence of ATP $\gamma$ S. **d-f**, Distribution of numbers of CMG diffraction-limited spots for DNA molecules imaged in **d**, the presence of ATP, **e**, the absence of nucleotide or, **f**, the presence of ATP $\gamma$ S. **g-i**, Distribution of numbers of CMG complexes within each diffraction limited spot on DNA molecules imaged in **g**, the presence of ATP, **h**, the absence of nucleotide or, **i**, the presence of ATP $\gamma$ S. **j-l**, Distribution of numbers of CMG complexes per DNA for DNA molecules imaged in **j**, the presence of ATP, **k**, the absence of nucleotide or, **l**, the presence of ATP $\gamma$ S.



**Supplementary Figure 5 | Mobility determination and motion classification of fluorescent spots imaged under different biochemical conditions.** **a**, Distribution of instantaneous velocities coming from the CPA fits of CMG spots in the presence of ATP; red lines show the instantaneous velocity cutoff ( $5\sigma_{\text{dCas9}}$ ) used to separate CMG spots into static or mobile. **b**, Distribution of anomalous coefficients  $\alpha$  of mobile CMG spots in the presence of ATP. **c**, Fraction of CMG spots imaged in the presence of ATP classified into static, subdiffusive, diffusive or unidirectionally moving ( $N_{\text{spots}}=43$ ); error bars show the standard error of proportion. **d**, Distribution of instantaneous velocities coming from the CPA fits of CMG spots in the absence of nucleotide; red lines show the instantaneous velocity cutoff ( $5\sigma_{\text{dCas9}}$ ) used to separate CMG spots into static or mobile. **e**, Distribution of anomalous coefficients  $\alpha$  of mobile CMG spots in the absence of nucleotide. **f**, Fraction of CMG spots imaged in the absence of nucleotide classified into static, subdiffusive, diffusive or unidirectionally moving ( $N_{\text{spots}}=36$ ); error bars show the standard error of proportion. **g**, Distribution of instantaneous velocities coming from the CPA fits of CMG spots in the presence of ATPyS; red lines show the instantaneous velocity cutoff ( $5\sigma_{\text{dCas9}}$ ) used to separate CMG spots into static or mobile. **h**, Distribution of anomalous coefficients  $\alpha$  of mobile CMG spots in the presence of ATPyS. **i**, Fraction of CMG spots imaged in the presence of ATPyS classified into static, subdiffusive, diffusive or unidirectionally moving ( $N_{\text{spots}}=34$ ); error bars show the standard error of proportion. **j**, (*same as inset in Fig. 2a*) Distribution of instantaneous velocities coming from the CPA fits of dCas9<sup>LD555</sup> spots; red lines show the instantaneous velocity cutoff ( $5\sigma_{\text{dCas9}}$ ) used to separate CMG spots into static or mobile. **k**, Fraction of dCas9<sup>LD555</sup> spots classified into static, subdiffusive, diffusive or unidirectionally moving ( $N_{\text{spots}}=23$ ). **l**, (left half) Diffusion constants of spots classified as diffusive for the different biochemical conditions tested (mean  $D$   $\pm$  standard deviation); (right half) Diffusion constants of spots classified as static for the different biochemical conditions tested (mean  $D$   $\pm$  standard deviation).

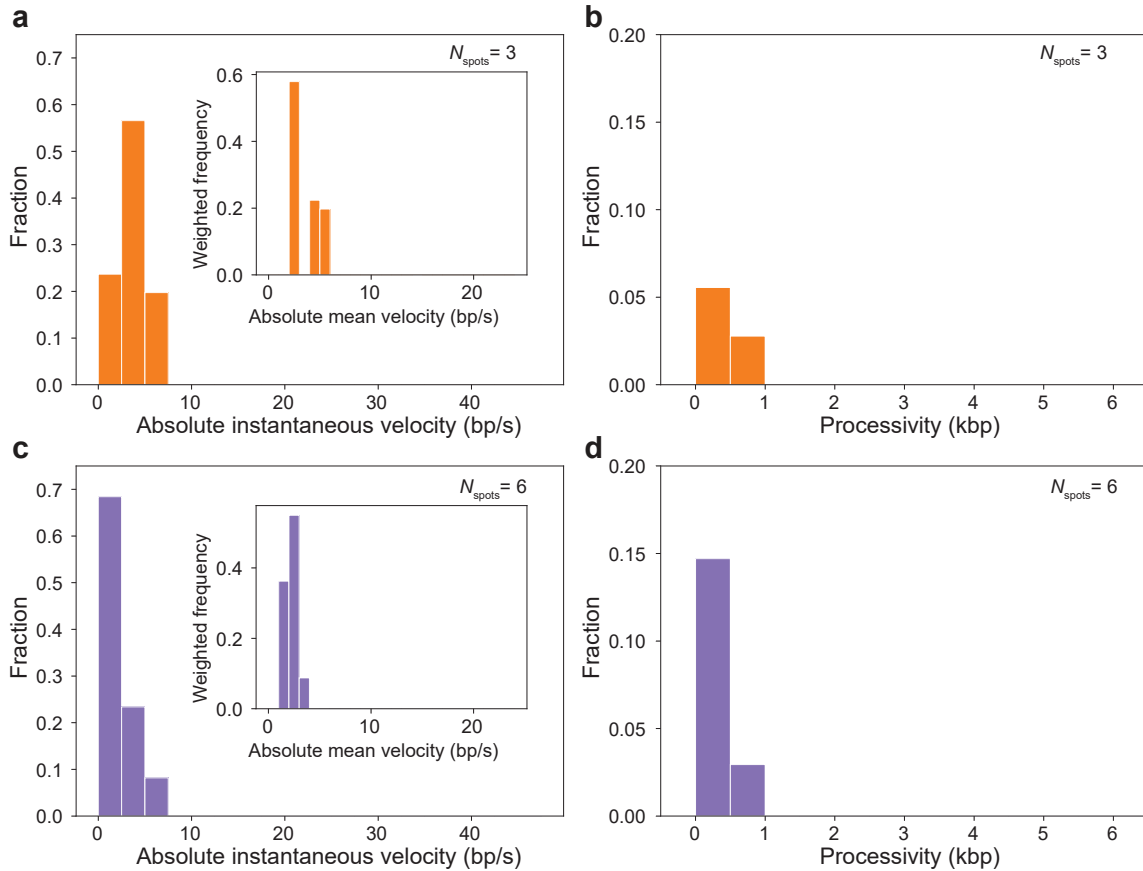


**Supplementary Figure 6 | Motion classification of simulated unidirectional or diffusive traces and anomalous diffusion exponent error determination.** Motion classification of simulated **a**, unidirectionally translocating traces with a representative velocity (5 bp/s) and **b**, diffusive traces with a representative diffusion coefficient ( $1.5 \times 10^{-3}$  kb<sup>2</sup>/s). **c**, Error determination of the anomalous diffusion exponent  $\alpha$  as a function of the minimum trace length; the error falls below 0.5 for a minimum trace length of 14 frames. We start with 512 traces of each motion type with a minimum trace length of 8 pulled from a population with a mean fluorophore lifetime of 25 frames, and gradually increase the trace length filtering. The traces used in **a-b**, are those with a minimum trace length of 14, to mirror the motion analysis done on experimentally obtained CMG spots.

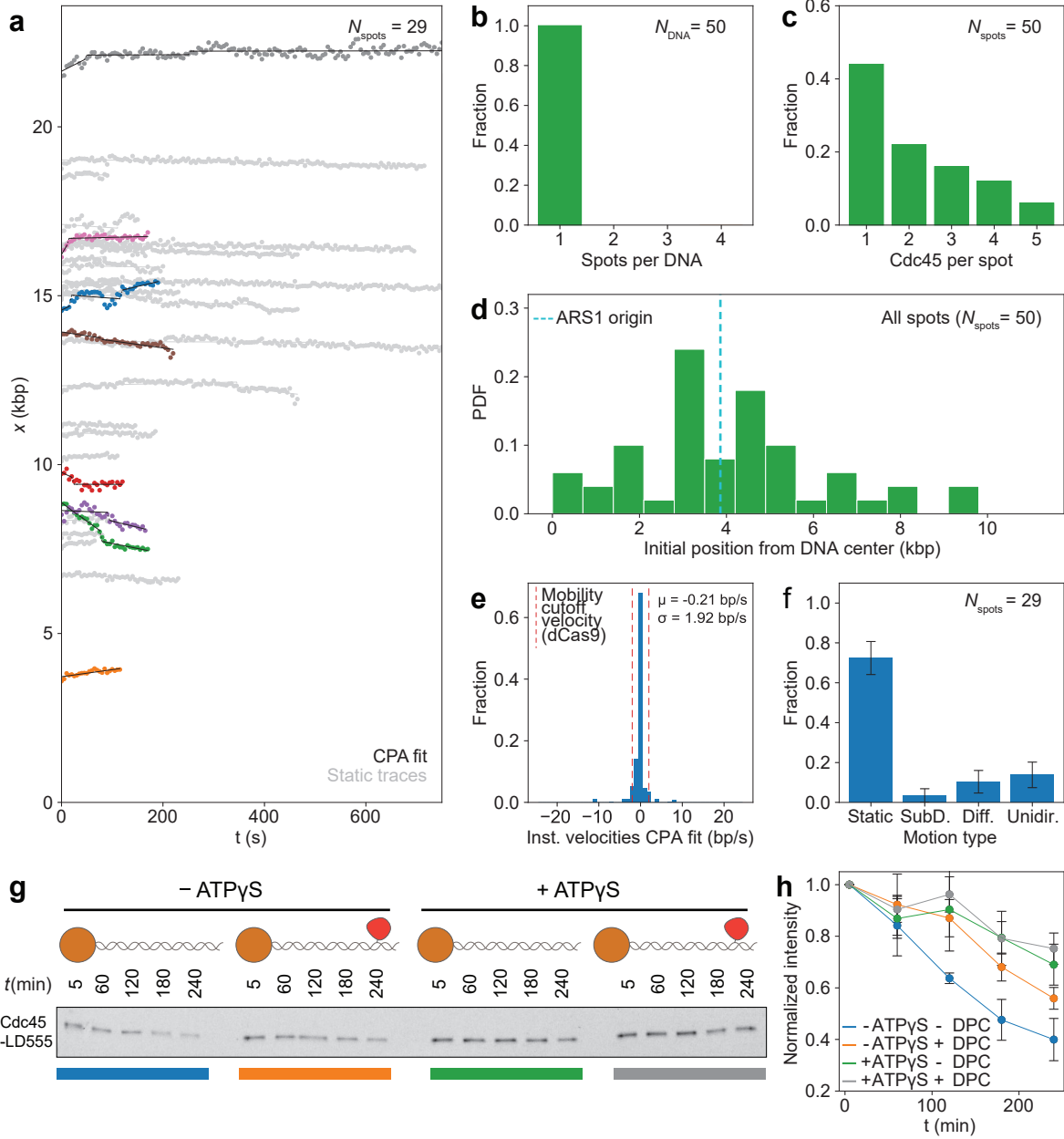


**Supplementary Figure 7 | Distribution of number of Cdc45 molecules per mobile diffraction-limited spot for the different biochemical conditions tested. a-c**, Distribution of number of Cdc45 molecules within diffraction-limited spots classified as unidirectionally-moving in the **a**, presence of ATP, **b**, absence of nucleotide or **c**, presence of ATP $\gamma$ S. **d-e**, Distribution of number of Cdc45 molecules within diffraction-limited spots classified as diffusively-moving in the **d**, presence of ATP or **e**, absence of nucleotide. **f-g**, Distribution of number of Cdc45 molecules within diffraction-limited spots classified as subdiffusively-moving in the **f**, presence of ATP or **g**, absence of nucleotide.



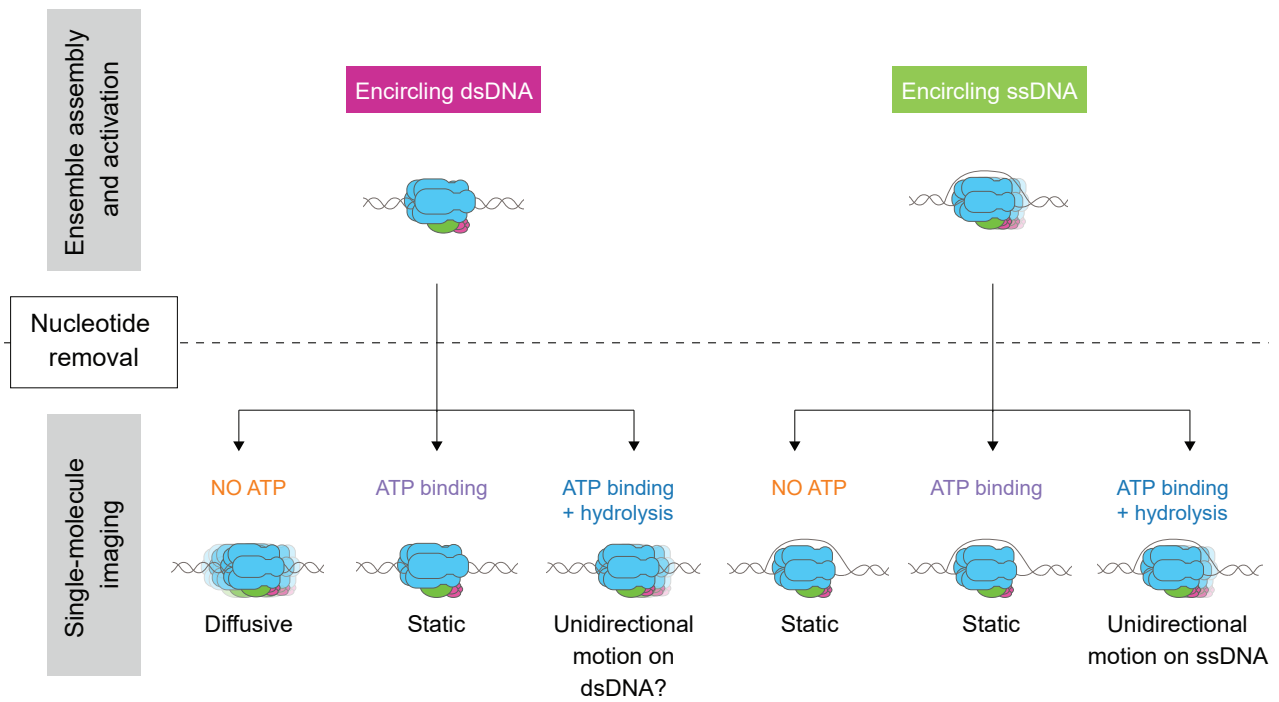


**Supplementary Figure 8 | Analysis of unidirectionally moving CMG under different biochemical conditions.** **a**, Distribution of absolute instantaneous velocities of unidirectionally moving CMG spots in the absence of nucleotide; (inset) Distribution of absolute mean velocities of unidirectionally moving CMG spots in the absence of nucleotide normalized by the length of each trace. **b**, Distribution of processivities of unidirectionally moving CMG spots in the absence of nucleotide. **c**, Distribution of absolute instantaneous velocities of unidirectionally moving CMG spots in the presence of ATP $\gamma$ S; (inset) Distribution of absolute mean velocities of unidirectionally moving CMG spots in the presence of ATP $\gamma$ S normalized by the length of each trace. **d**, Distribution of processivities of unidirectionally moving CMG spots in the presence of ATP $\gamma$ S.



**Supplementary Figure 9 | Nucleotide binding halts CMG diffusion independently of DNA melting.**

**a**, Position vs. time plots of  $\text{CMG}^{\text{Mcm2(6A)}}$  spots in the presence of ATP; CPA fits are plotted in black, static traces are shown in light gray and mobile traces are shown in all other colors. **b**, Distribution of numbers of  $\text{CMG}^{\text{Mcm2(6A)}}$  diffraction-limited spots per DNA. **c**, Distribution of numbers of  $\text{CMG}^{\text{Mcm2(6A)}}$  complexes within each diffraction-limited spot. **d**, Distribution of initial positions on the DNA of all  $\text{CMG}^{\text{Mcm2(6A)}}$  diffraction-limited spots. **e**, Distribution of instantaneous velocities coming from the CPA fits of  $\text{CMG}^{\text{Mcm2(6A)}}$  spots in the presence of ATP; red lines show the instantaneous velocity cutoff ( $5\sigma_{\text{dCas9}}$ ) used to separate  $\text{CMG}^{\text{Mcm2(6A)}}$  spots into static or mobile. **f**, Fraction of  $\text{CMG}^{\text{Mcm2(6A)}}$  spots imaged in the presence of ATP classified into static, subdiffusive, diffusive or unidirectionally moving ( $N_{\text{spots}}=29$ ); error bars show the standard error of proportion. **g**, Fluorescent scan of an SDS-PAGE gel showing the amount of  $\text{Cdc45}^{\text{LD555}}$  left on linear DNA bound to magnetic beads at one end and containing either a free end or an end capped with a covalently crosslinked methyltransferase. **h**, Densitometry quantification of the experiment shown in **g**, showing the average normalized intensity of three replicates together with their standard deviation. Data points are connected by solid lines to guide the eye. Source data are provided as a Source Data file.



**Supplementary Figure 10 | Final model.** Model showing all the experimental outcomes observed in this study with different potential explanations.

## Supplementary Tables:

Supplementary Table 1: oligos and primers used in this study

Name	5' to 3' sequence
DRM_005	GCTGCGCCTGCTGAACGGTGATTATAAAGATGATGATGGG
DRM_006	AGCCAGCTCAGGCTATCGCCCTCGTCTGTGACTTCATC
DRM_184	ACGGCTGTAAATGGGGGGAGTGATAAGAAATACTCAATAGGC
DRM_185	AATAACCAACTTAATGAATCCCCCACGTGATGATGATGATG
TL_033	GCGCGCCAATTGGAGCTCCACCGCGG
TL_034	GGCGCGCCGAAACAGCTATGACCATGATTACGCC
DRM_218	ATACTTTAGATTGATTTTC[5-Fluoro-2'-dC]GGCTTCACCTG
DRM_220	ATACTTTAGATTGATTTCCGGCTTCACCTG
DRM_222	Biotin-CTAGTGGATCCCCAGGGCT

Supplementary Table 2: gBlocks™ used in this study

gBlock™	5' to 3' Sequence
gBlock™ DRM8	<p>TCATTCTGAGAATAGTGTATGCGGCGACCGAGTTGCTCTTGCCTGGCGTCAATAC  GGGATAATACCGCGCCACATAGCAGAACTTTAAAAGTGCTCATCATTGGAAAACGT  TCTTCGGGGCGAAAACCTCTCAAGGATCTTACCGCTGTTGAGATCCAGTTCGATGTA  ACCCACTCGTGCACCCAACCTGATCTTCAGCATCTTTTACTTTACCCAGCGTTTCTG  GGTGAGCAAAAACAGGAAGGCAAAATGCCGCAAAAAAGGGAATAAGGGCGACAC  GGAAATGTTGAATACTCATACTCTTCTTTTTCAATATTATTGAAGCATTATCAGG  GTTATTGTCTCATGAGCGGATACATATTTGAATGTATTTAGAAAAATAAACAAATAG  GGTTCCGCGCACATTTCCCGAAAAGTGCCACCTAAATTGAAGCGTTAATATTT  TGTTAAAATTTCGGTTAAATTTTTGTTAAATCAGCTCATTTTTTAAACCAATAGGCCGA  AATCGGCATAATCCCTTATAAATCAAAGAATAGACCGAGATAGGGTTGAGTGTG  TTCCAGTTTGGAAACAAGAGTCCACTATTAAGAACGTGGACTCCAACGTCAAAGGG  CGAAAAACCGTCTATCAGGGCGATGGCCACTACGTGAACCATCACCTAATCAA  GTTTTTTGGGGTCGAGGTGCCGTAAGCACTAAATCGGAACCCTAAAGGGAGCCC  CCGATTTAGAGCTTGACGGGGAAAGCCCGCAACGTGGCGAGAAAGGAAGGGAA  GAAAGCGAAAGGAGCGGGCGCTAGGGCGCTGGCAAGTGTAGCGGTCACGCTGC  GCGTAACCACCACACCCGCCGCGCTTAATGCGCCGCTACAGGGCGCGTCCCATT  CGCCATTGCTGAGGCGCAACTGTTGGGAAGGGCGATCGGTGCGGGCCTCTTCGC  TATTACGCCAGCTGGCGAAAGGGGATGTGCTGCAAGGCGATTAAGTTGGGTAAAC  GCCAGGTTTTCCAGTCACGACGTTGTAAAACGACGGCCAGTGAATTGTAATAC  GACTCACTATAGGGCGAATTGAGCTCCACCGCGGTGGCGGGCGCTCTAGAACT  AGTGGATCCCCAGGGCTGCAGGAATTCGAGCTCGGTACCCACAATCAATCAAAAA  GCCAAATGATTTAGCATTATCTTTACATCTTGTTATTTTACAGATTTTATGTTTAGAT  CTTTTATGCTTGCTTTTTCAAAGGCCTGCAGGCAAGTGCACAAACAATACTTAAATA  AATACTACTCAGTAATAACCTATTTCTTAGCATTTTTGACGAAATTTGCTATTTTTGTT  AGAGTGGGGATCCTCTAGAGTCGACCTGCAGGCATGCAAGCTTATCGATACCGTC  GACCTCGAGGGGGGGCACGGTACCAGCTTTTGTCCCTTTAGTGAGGGTTAATTT  CGAGCTTGGCGTAATCATGGTCATAGCTGTTTCCTGTGTGAAATTGTTATCCGCTC  ACAATCCACACAACATACGAGCCTGAAGCATAAAGTGTAAGCCTGGGGTGCCT  AATGAGTGAGCTAACTACAACCTCAGCTTTCGCTCACTGCCCGCTTTCCAGTCCG  GGAAACCTGTGCGTCCAGCTGCATTAATGAATCGGCCAACGCGCGGGGAGAGGC  GGTTTGCGTATTGGGCGCTCTTCCGCTTCCGCTCACTGACTCGCTGCGCTCGG  TCGTTCCGGCTGCGGCGAGCGGTATCAGCTCACTCAAAGGCGGTAATACGGTTATC  CACAGAATCAGGGGATAACGCAGGAAAGAACATGTGAGCAAAAGGCCAGCAAAAG  GCCAGGAACCGTAAAAAGGCCGCGTTGCTGGCGTTTTTCCATAGGCTCCGCCCCC  CTGACGAGCATCACAAAAATCGACGCTCAAGTCAGAGGTGGCGAAACCCGACAGG  ACTATAAAGATAACCAGGCGTTTTCCCCTGGAAGCTCCCTCGTGCGCTCTCCTGTT  CGACCCTGCCGCTTAACGGATACCTGTCCGCCTTTCTCCCTTCGGGAAGCGTGGC  GCTTTCTCATAGCTCACGCTGTAGGTATCTCAGTTCGGTGTAGGTGCTTCGTTCCA  AGCTGGGCTGTGTGCACGAAAACAGGATTAGCAGAGCGAGGTATGTAGGCGGTG  CTACAGAGTTCTTGAAGTGTTGGCCTAACTACGGCTACACTAGAAGGACAGTATTT  GGTATCTGCGCTCTGCTGAAGCCAGTTACCTTCGGAAAAAGAGTTGGTAGCTCTT  GATTCGGCAAACATACCAACGCTGGTAGCGGTAGTATTTTTGTTTGAAGCAGCAG  ATTACGCGCAGAAAAAAGGATCTCAAGATGATCCTTTGATCTTTTCTACGGGGTC  TGACGCTCAGTGAACGAAAACCTCACGTTAAGGGATATTGGTCATGAGATTATCAA  AATGGATCTTCACCTAGATCCTTTTAAATTACAGGTGAAGCCGGAAATCAATCTAAA  GTAT</p>